

## Second mode unstable disturbance measurement of hypersonic boundary layer on cone by wavelet transform

Jian Han · Nan Jiang · Yan Tian

Received: 27 January 2010 / Revised: 10 August 2010 / Accepted: 16 December 2010

©The Chinese Society of Theoretical and Applied Mechanics and Springer-Verlag Berlin Heidelberg 2011

**Abstract** Experimental investigation of hypersonic boundary layer instability on a cone is performed at Mach number 6 in a hypersonic wind tunnel. Time series signals of instantaneous fluctuating surface-thermal-flux are measured by Pt-thin-film thermocouple temperature sensors mounted at 28 stations on the cone surface in the streamwise direction to investigate the development of the unstable disturbance. Wavelet transform is employed as a mathematical tool to obtain the multi-scale characteristics of fluctuating surface-thermal-flux both in the temporal and spectrum space. The conditional sampling algorithm using wavelet coefficient as an index is put forward to extract the unstable disturbance waveform from the fluctuating surface-thermal-flux signals.

The project was supported by the National Natural Science Foundation of China (10832001, 10872145), Opening subject of State Key Laboratory of Nonlinear Mechanics, Institute of Mechanics, Chinese Academy of Sciences.

J. Han (✉)  
Department of Mathematics, Tianjin University,  
300072 Tianjin, China  
e-mail: hanjian@tju.edu.cn

J. Han · N. Jiang · Y. Tian  
Department of Mechanics, Tianjin University,  
300072 Tianjin, China  
e-mail: nanj@tju.edu.cn

N. Jiang · Y. Tian  
Tianjin Key Laboratory of Modern Engineering Mechanics,  
300072 Tianjin, China

N. Jiang  
State Key Laboratory of Nonlinear Mechanics,  
Institute of Mechanics,  
Chinese Academy of Sciences, 100190 Beijing, China

The generic waveform for the second mode unstable disturbance is obtained by a phase-averaging technique. The development of the unstable disturbance in the streamwise direction is assessed both in the temporal and spectrum space. Our study shows that the local unstable disturbance detection method based on wavelet transformation offers an alternative powerful tool in studying the hypersonic unstable mode of laminar-turbulent transition. It is demonstrated that, at hypersonic speeds, the dominant flow instability is the second mode, which governs the course of laminar-turbulent transition of sharp cone boundary layer.

**Keywords** Hypersonic boundary layer · Sharp cone · Instability · Wavelet transform

### 1 Introduction

Hypersonic boundary layer instability and laminar-turbulent transition is one of the most important problems in aeronautic and astronautic engineering as it is characterized by attendant increases in wall heat transfer and skin friction drag of hypersonic vehicles [1]. These increases have significant impact on the performance control, fuel consumption, structural design and thermal protection system of hypersonic vehicles because the aerodynamics performances are very sensitive to the changes in wall thermal and aerodynamic loadings that accompany laminar-turbulent transition. Therefore, understanding the laminar-turbulent transition mechanism and predicting the transition location accurately are the keys to achieve the desired aerodynamic performances [2]. Unlike the case of subsonic flow, the mechanisms underlying the laminar-turbulence transition in hypersonic flow still remain poorly understood both in experiment and theory [3]. The uncertainty in the prediction of the transition location results in overly conservative designs that are not optimally efficient in the budget of propulsion and payload capacity.

At hypersonic velocities, for Mach numbers greater than 4–4.5, the dominant disturbance are termed the Mach mode. The Mach mode is an inviscid instability that is driven by a region of mean flow and is supersonic relative to the disturbance phase velocity. Besides the first vortex instability for the Mach mode, there arises a new, acoustic type of instability (the so-called second mode instability) [4]. Demetriades [5], Kendall [6], Stetson et al. [7] were among the first to find the Mach mode in experiments, while Kimmel et al. [8], Lachowicz et al. [9], and Doggett et al. [10] also observed the second mode later in their experiments separately. According to theoretical and numerical studies, the second mode in hypersonic flows is the dominant instability and is expected to govern the occurrence and development of laminar-turbulent transition [11]. Therefore, identifying and understanding the second mode mechanism is of considerable importance. However, in the experimental measurements, it is difficult to distinguish the second Mach mode from the large-bandwidth high frequency background [12].

Wavelet transform [13] is a relatively new digital signal processing technique that combines the dual time-frequency analysis of unstationary signals with enormous applications in many fields of science and engineering. The wavelet transform employs an analytic basis function named mother wavelet and convolutes time series signals with the mother wavelet function at a definite time and a definite scale by means of dilations and translations of mother wavelet. It provides a two-dimensional unfolding of one-dimensional signals resolving both on the time and the temporal scale as independent variables. So this method comprises a decomposition of signals both on time and scale plane simultaneously. The ability of displaying both time and frequency information for wavelet transform makes it well suited for isolating the Mach mode disturbance causing hypersonic boundary layer transition from experimental transient measured signals.

## 2 Experimental technique

The experiment is conducted in a hypersonic blow-down wind tunnel. This tunnel is designed for the Mach numbers  $M_\infty = 5\text{--}15$  and the unit Reynolds numbers  $Re_1 = (5 \times 10^5 \text{--} 7 \times 10^7) \text{ m}^{-1}$ ; There is a set of changeable profiled and conic axis-symmetric nozzles. An ohmic heater is used for maintaining air temperature in the settling chamber up to 700–1 300 K. The open-jet test section has the length of 1 600 mm with the nozzle end diameter of 480 mm. The stagnation pressure  $P_0$  and stagnation temperature  $T_0$  were measured during the run and kept at constant. All the results of  $P_0$  measurements were within the range of no more than 2.69 MPa. The stagnation temperature  $T_0$  was 702 K. The unit Reynolds numbers  $Re_1 = 1.3 \times 10^7 \text{ m}^{-1}$ .

The model is a 5° half-angle sharp cone of 600 mm in length. It consists of a sharp cone nose of 1 mm in blunt-

ness radius and the base part equipped with 28 Pt-thin-film thermocouple sensors to measure the wall temperature. The thermocouple sensors are located along the bottom generatrix. First thermocouple is located at 90 mm from the cone apex; the other ones are situated with uniform spatial separation from each other along a bottom generatrix in streamwise direction.

The output signals were digitized by 12 bit analog-to-digital converter data acquisition card with  $\pm 5$  V range and 1MHz sampling rate. At each station of measurement 524 288 samples are recorded.

## 3 Experimental data processing method

Relative to an analytic basis function termed mother wavelet  $\psi(t)$ ,  $\psi_{ab}(t)$  is the shift (by factor  $b$ ) and dilatation (by factor  $a$ ) of  $\psi(t)$

$$\psi_{ab}(t) = \frac{1}{\sqrt{a}} \psi\left(\frac{t-b}{a}\right), \quad \text{with } a, b \in \mathbf{R} \text{ and } a > 0. \quad (1)$$

The continuous wavelet transform of signal  $f(t)$  with respect to a set of wavelet  $\psi_{ab}(t)$  for different factors  $b$  and  $a$  is defined as their inner product

$$\psi_f(a, b) = \int_{-\infty}^{+\infty} f(t) \overline{\psi_{ab}(t)} dt, \quad (2)$$

where “—” indicates the complex conjugate operator. Wavelet analysis is an extension of the Fourier analysis by shift time windows with proper time interval (window width). This is appropriate for spectrum analysis of non-stationary signals with multi-scale local disturbance and singular structure whose power spectral characteristic is simultaneous in time [14]. The occurring positions and scale of local disturbance can be identified accurately by wavelet analysis. As a new tool, wavelet transform can be devoted to identifying singular structure in time series signals by presetting a conditional threshold level on wavelet coefficients [15]. If the wavelet coefficient satisfies the sampling conditions (its modulus is exceeding the threshold level), the wavelet coefficient will be preserved, which means the wavelet coefficient is in the incidence of the singular structure. Otherwise, the wavelet coefficient will be set to zero, which means that the wavelet coefficient is independent of the singular structure [16].

$$\psi_{f_s}(a, b) = \begin{cases} \psi_f(a, b), & \text{if } |\psi_f(a, b)| > L, \\ 0, & \text{otherwise.} \end{cases} \quad (3)$$

The singular structure segments can be recovered from the preserved wavelet coefficients by wavelet inverse transformation.

$$f_s(t) = \frac{2}{C_\psi} \int_0^{+\infty} \frac{1}{a^2} \int_{-\infty}^{+\infty} \psi_{f_s}(a, b) \overline{\psi_{ab}(t)} db da. \quad (4)$$

Once the transient signatures have been segmented from the

experimental output signals, the eigenfunction waveform of the universal signature signals can be obtained by superposition and average these conditional sampled signals

$$\langle f(t) \rangle = \frac{1}{N} \sum_{i=1}^N f_s(b_i + t), \quad t \in [-a, a]. \quad (5)$$

#### 4 Experimental results

Figure 1 shows the wavelet coefficient magnitude contour of the temperature signals at different stations along one generatrix. The corresponding acquired wall thermal flux signals and the unstable disturbance signals extracted from the ac-

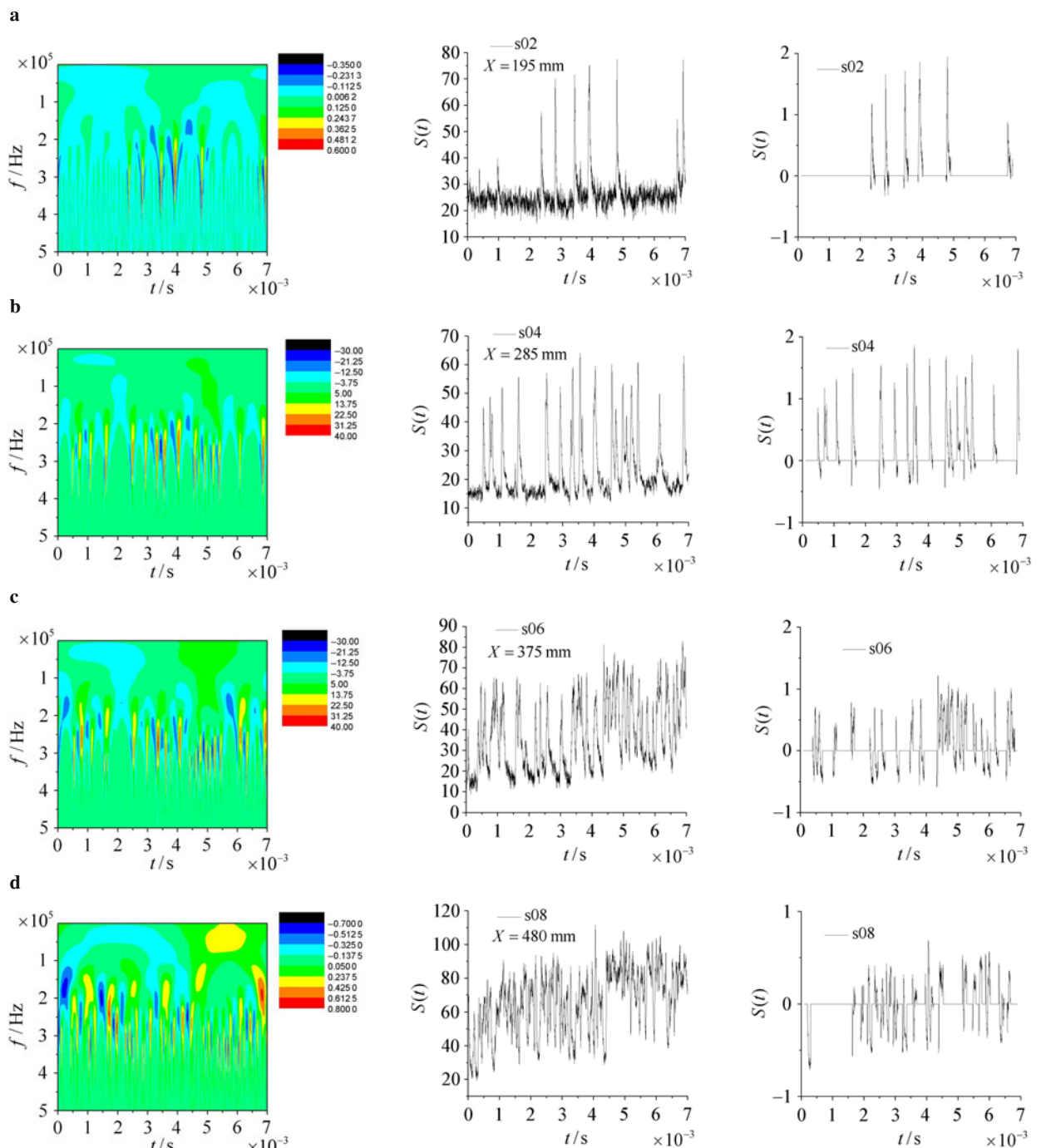


**Fig. 1** The wavelet coefficient magnitude contour (left), signals (middle) and the corresponding unstable disturbance (right) extracted from the signals by wavelet inverse transform at different stations along one generatrix on the cone surface. **a**  $X = 195$  mm; **b**  $X = 285$  mm; **c**  $X = 375$  mm; **d**  $X = 480$  mm

quired signals by wavelet inverse transformation (4) are also presented in the same figure to compare the disturbance occurrence locations. From the plane representation of the wavelet coefficients, it can be seen that some local high magnitudes of the wavelet coefficients exist at different times in the scale range of 200 kHz to 300 kHz pointing out the disturbance corresponding to the second-mode. The second mode disturbance is dominant in a hypersonic laminar boundary layer. More and more large-amplitude disturbances are triggered downstream involving mode nonlinear interaction of the disturbance. And then at the last station  $X = 480$  mm, the disturbance is fully developed and the transition reach its peak. It can be seen that there exist some local high-magnitude unstable disturbances occurring at different times. More and more large-amplitude unstable disturbances ensue downstream with the development of the instability.

A conditional phase-averaging method has been proposed for obtaining the universal eigenfunction waveform

of the unstable disturbance. Therefore a detection and segmentation algorithm has been developed. First it searches for wavelet coefficient values that reach its maximum, and then a segment of the fluctuating surface-thermal-flux signals centering at the time that corresponding to the wavelet coefficient maximum index is cut out of with a certain time scale length. All the segments around all found unstable disturbances have been superposed and averaged for gaining a universal eigen-waveform of the unstable disturbance. Figure 2 shows the conditional phase-averaging waveform of the second mode unstable disturbances at 8 stations. It can be seen that the second mode unstable disturbance develops at the beginning with its amplitude grows gradually. The magnitude reaches its peak at the 3rd station where  $X = 240$  mm. From then on, the magnitude begins to decrease and its shapes change from anti-symmetric to symmetric.

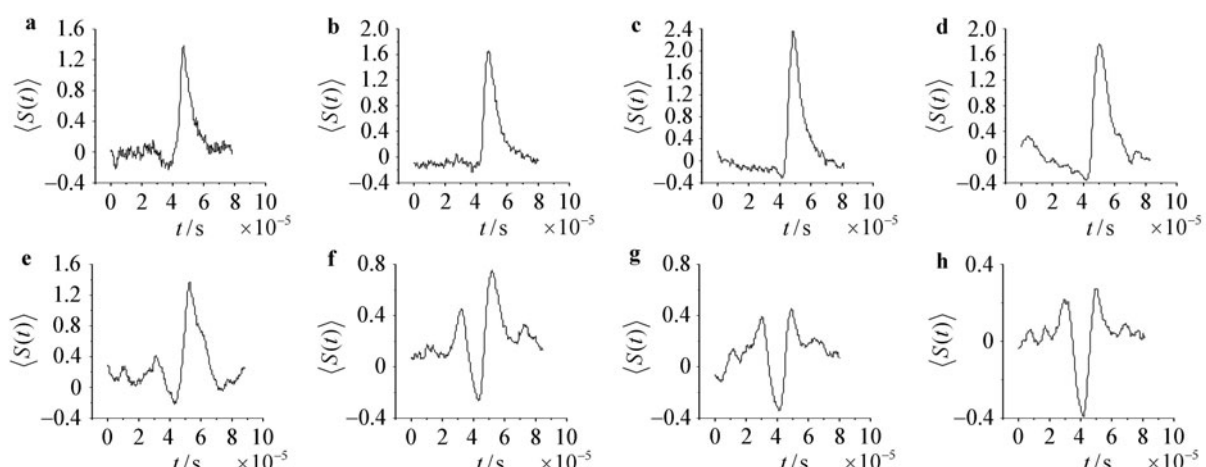


**Fig. 2** Conditional phase-averaging generic waveform for the second mode unstable disturbances at 8 stations along one generatrix on the cone surface. **a**  $X = 165$  mm; **b**  $X = 195$  mm; **c**  $X = 240$  mm; **d**  $X = 285$  mm; **e**  $X = 330$  mm; **f**  $X = 375$  mm; **g**  $X = 420$  mm; **h**  $X = 480$  mm

The power spectrum that is calculated for the extracted unstable disturbance signals and presented in Fig. 3 provides

developing details of the unstable disturbance in the spectrum space. At the initial stage of transition, there is no signif-

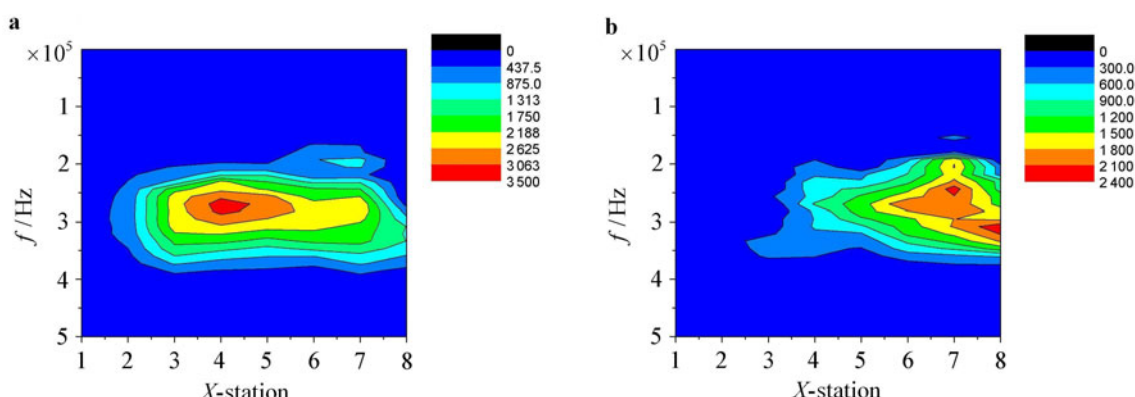


**Fig. 3** Power spectrum of the extracted unstable disturbance at 8 stations along one generatrix on the cone surface. 1:  $X = 165$  mm, 2:  $X = 195$  mm, 3:  $X = 240$  mm, 4:  $X = 285$  mm, 5:  $X = 330$  mm, 6:  $X = 375$  mm, 7:  $X = 420$  mm, 8:  $X = 480$  mm

ficant frequency in the spectrum while the second mode gradually develops from  $X = 195$  mm. With the development of the unstable disturbance, the second mode becomes dominant with its amplitude growing quickly. The significant frequency peak is observed at the 4th station where  $X = 285$  mm. The dominant frequency band center is  $f = 270$  kHz including the second mode at this station. This means that the unstable disturbance is fully developed and the hypersonic boundary layer begins to transit from laminar to turbulence. The second mode begins to decay at the 7th or 8th station where  $X$  is 420 mm or 480 mm. This implies that the transition reaches its peak. Our results are in consistent with Nodaona Chokani's [12] conclusion shown in Fig. 4. Figure 4 shows the second mode is centered at  $f = 280$  kHz for the adiabatic wall which is very close to our results. Our results also support Lachowicz et al.'s [9] conclusion that the dominant instability is quite pronounced at  $f = 230$  kHz for the most amplified Mach mode in the transitioning hypersonic laminar boundary layer (Fig. 5).

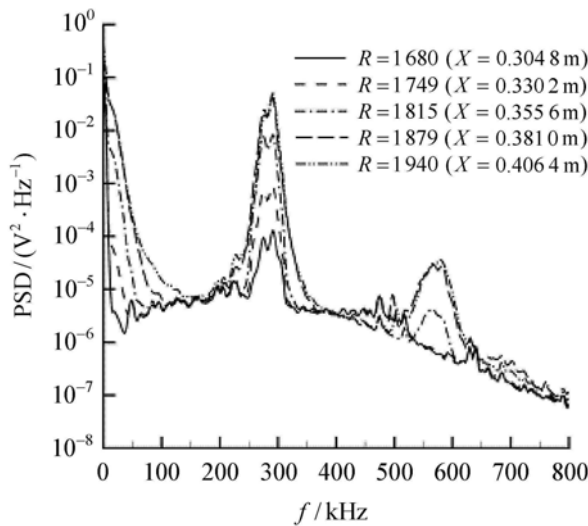


**Fig. 4** Streamwise evolution of power spectral density on adiabatic wall [12]

## 5 Conclusion

A new analysis method based on wavelet transform is presented for investigating the evolution mechanism of the second mode unstable disturbance during the hypersonic boundary layer transition. The local unstable disturbance detection method based on wavelet transformation is a powerful tool in studying the laminar-turbulent transition. The second mode instability of the disturbance is demonstrated to be the important mechanism in the course of hypersonic boundary layer laminar-turbulent transition. At hypersonic speeds, the dominant flow instability is the second mode, which gov-

erns the course of laminar-turbulent transition of sharp cone boundary layer. This second mode instability precedes the final breakdown of the hypersonic laminar boundary layer and transition to turbulence.

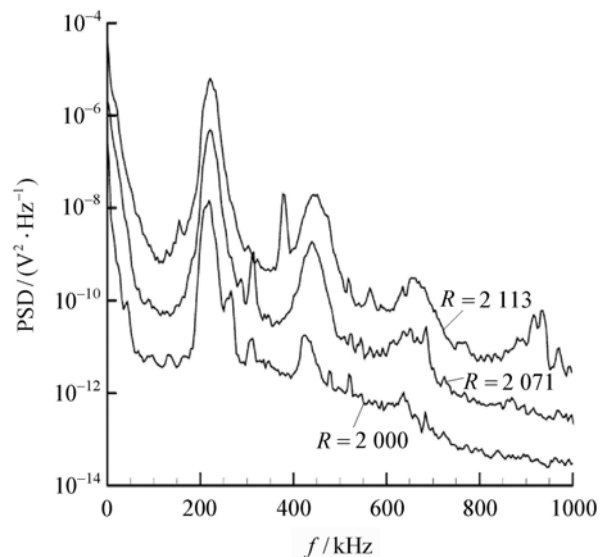


**Fig. 5** Evolution of the power spectral density on the Lachowicz fared-cone model. For the sake of clarity, successive spectra are offset by one decade. The frequency of the most amplified Mach mode is 230 kHz [2]

**Acknowledgments** The authors gratefully acknowledge the China Aerodynamics Technique Research Academy for supporting the experiment and providing the experiment data.

## References

- 1 Ferrier, M., Chokani, N.: Hypersonic transition detection with single point hot-wire measurements. AIAA paper, 2003-0063
- 2 Chokani, N.: VITA measurements of transition in transitional hypersonic boundary layer flows. *Experiments in Fluids* **38**(4), 440–448 (2005)
- 3 Gurley, K., Kijewski, T., Kareem, A.: First- and higher-order correlation detection using wavelet transforms. *Journal of Engineering Mechanics* **129**(2), 188–201 (2003)
- 4 Maslov, A.A., Shiplyuk, A.N., Bountin, D.A., et al.: Mach 6 boundary-layer stability experiments on sharp and blunted cones. *Journal of Spacecraft and Rockets* **43**(1), 71–76 (2006)
- 5 Demetriades, A.: New experiments on hypersonic boundary layer stability including wall temperature effects. In: Proc. Heat Transfer Fluid Mechanic Institute **26**, 39–54 (1978)
- 6 Kendall, J.M.: Wind tunnel experiments relating to supersonic and hypersonic boundary layer transition. *AIAA Journal* **13**, 290–299 (1975)
- 7 Stetson, K.F., Thompson, E.R., Donaldson, J.C., et al.: Laminar boundary layer stability experiments on a cone at Mach 8. Part 1: Sharp cone. *AIAA Paper 83-1761* (1983)

- 8 Kimmel, R.L., Demetriades, A., Donaldson, J.C.: Space-time correlation measurements in a hypersonic transitional boundary layer. *AIAA Journal* **34**, 2484–2489 (1996)
- 9 Lachowicz, J.T., Chokani, N., Wilkinson, S.P.: Boundary-layer stability measurements in a hypersonic quiet tunnel. *AIAA Journal* **34**, 2496–2500 (1996)
- 10 Doggett, G.P., Wilkinson, S.P., Chokani, N.: Effects of angle of attack on hypersonic boundary layer stability in a quiet wind tunnel. *AIAA Journal* **35**(3), 464–470 (1997)
- 11 Chokani, N.: Perspective: Stability experiments at hypersonic speeds in a quiet wind tunnel. *AIAA Paper*, 2001-0211
- 12 Chokani, N.: Nonlinear evolution of Mach modes in a hypersonic boundary layer. *Physics of Fluids* **17**(1), 14102–14114 (2005)
- 13 Chokani, N.: Nonlinear spectral dynamics of hypersonic laminar boundary layer flow. *Physics of Fluids* **11**(12), 3846–3851 (1999)
- 14 Norris, J.D., Chokani, N.: Transient nonlinear interactions in a hypersonic laminar boundary layer. *AIAA Paper*, 2002-0154
- 15 Jiang, N., Zhang, J.: Detecting multi-scale coherent eddy structures and intermittency in turbulent boundary layer by wavelet analysis. *Chinese Physics Letters* **22**(8), 1968–1971 (2005)
- 16 Liu, J.H., Jiang, N.: Two phases of coherent structure motions in turbulent boundary layer. *Chinese Physics Letters* **24**(9), 2617–2620 (2007)